Journal club cryo-EM

PNAS PNAS PNAS

Structure of β-galactosidase at 3.2-Å resolution obtained by cryo-electron microscopy

Alberto Bartesaghi[1], Doreen Matthies[1], Soojay Banerjee, Alan Merk, and Sriram Subramaniam[2]

Laboratory of Cell Biology, Center for Cancer Research, National Cancer Institute, National Institutes of Health, Bethesda, MD 20892

Edited by Wah Chiu, Baylor College of Medicine, Houston, TX, and approved June 20, 2014 (received for review February 14, 2014)

We report the solution structure of *Escherichia coli* β-galactosidase (~465 kDa), solved at ~3.2-Å resolution by using single-particle cryo-electron microscopy (cryo-EM). Densities for most side chains, including those of residues in the active site, and a catalytic Mg^{2+} ion can be discerned in the map obtained by cryo-EM. The atomic model derived from our cryo-EM analysis closely matches the 1.7-Å crystal structure with a global rmsd of ~0.66 Å. There are significant local differences throughout the protein, with clear evidence for conformational changes resulting from contact zones in the crystal lattice. Inspection of the map reveals that although densities for residues with positively charged and neutral side chains are well resolved, systematically weaker densities are observed for residues with negatively charged side chains. We show that the weaker densities for negatively charged residues arise from their greater sensitivity to radiation damage from electron irradiation as determined by comparison of density maps obtained by using electron doses ranging from 10 to 30 $e^-/Å^2$. In summary, we establish that it is feasible to use cryo-EM to determine near-atomic resolution structures of protein complexes (<500 kDa) with low symmetry, and that the residue-specific radiation damage that occurs with increasing electron dose can be monitored by using dose fractionation tools available with direct electron detector technology.

Science AAAS

ELECTRON MICROSCOPY

2.2 Å resolution cryo-EM structure of β-galactosidase in complex with a cell-permeant inhibitor

Alberto Bartesaghi,[1]* Alan Merk,[1]* Soojay Banerjee,[1] Doreen Matthies,[1] Xiongwu Wu,[2] Jacqueline L. S. Milne,[1] Sriram Subramaniam[1]†

Cryo–electron microscopy (cryo-EM) is rapidly emerging as a powerful tool for protein structure determination at high resolution. Here we report the structure of a complex between *Escherichia coli* β-galactosidase and the cell-permeant inhibitor phenylethyl β-D-thiogalactopyranoside (PETG), determined by cryo-EM at an average resolution of ~2.2 angstroms (Å). Besides the PETG ligand, we identified densities in the map for ~800 water molecules and for magnesium and sodium ions. Although it is likely that continued advances in detector technology may further enhance resolution, our findings demonstrate that preparation of specimens of adequate quality and intrinsic protein flexibility, rather than imaging or image-processing technologies, now represent the major bottlenecks to routinely achieving resolutions close to 2 Å using single-particle cryo-EM.

How to get a high-resolution structure ?

→ Sample preparation

→Microscope imaging

→ Data processing

Journal club cryo-EM

PNAS PNAS PNAS

Structure of β-galactosidase at 3.2-Å resolution obtained by cryo-electron microscopy

Alberto Bartesaghi[1], Doreen Matthies[1], Soojay Banerjee, Alan Merk, and Sriram Subramaniam[2]

Laboratory of Cell Biology, Center for Cancer Research, National Cancer Institute, National Institutes of Health, Bethesda, MD 20892

Edited by Wah Chiu, Baylor College of Medicine, Houston, TX, and approved June 20, 2014 (received for review February 14, 2014)

We report the solution structure of *Escherichia coli* β-galactosidase (~465 kDa), solved at ~3.2-Å resolution by using single-particle cryo-electron microscopy (cryo-EM). Densities for most side chains, including those of residues in the active site, and a catalytic Mg^{2+} ion can be discerned in the map obtained by cryo-EM. The atomic model derived from our cryo-EM analysis closely matches the 1.7-Å crystal structure with a global rmsd of ~0.66 Å. There are significant local differences throughout the protein, with clear evidence for conformational changes resulting from contact zones in the crystal lattice. Inspection of the map reveals that although densities for residues with positively charged and neutral side chains are well resolved, systematically weaker densities are observed for residues with negatively charged side chains. We show that the weaker densities for negatively charged residues arise from their greater sensitivity to radiation damage from electron irradiation as determined by comparison of density maps obtained by using electron doses ranging from 10 to 30 $e^-/Å^2$. In summary, we establish that it is feasible to use cryo-EM to determine near-atomic resolution structures of protein complexes (<500 kDa) with low symmetry, and that the residue-specific radiation damage that occurs with increasing electron dose can be monitored by using dose fractionation tools available with direct electron detector technology.

Science AAAS

ELECTRON MICROSCOPY

2.2 Å resolution cryo-EM structure of β-galactosidase in complex with a cell-permeant inhibitor

Alberto Bartesaghi,[1]* Alan Merk,[1]* Soojay Banerjee,[1] Doreen Matthies,[1] Xiongwu Wu,[2] Jacqueline L. S. Milne,[1] Sriram Subramaniam[1]†

Cryo–electron microscopy (cryo-EM) is rapidly emerging as a powerful tool for protein structure determination at high resolution. Here we report the structure of a complex between *Escherichia coli* β-galactosidase and the cell-permeant inhibitor phenylethyl β-D-thiogalactopyranoside (PETG), determined by cryo-EM at an average resolution of ~2.2 angstroms (Å). Besides the PETG ligand, we identified densities in the map for ~800 water molecules and for magnesium and sodium ions. Although it is likely that continued advances in detector technology may further enhance resolution, our findings demonstrate that preparation of specimens of adequate quality and intrinsic protein flexibility, rather than imaging or image-processing technologies, now represent the major bottlenecks to routinely achieving resolutions close to 2 Å using single-particle cryo-EM.

Background

- β-galactosidase : enzyme that catalyses the hydrolysis of lactose and many other β-galactosides into monosaccharides
- 465 kDa (tetramer)
- Solved by cryo-EM at 3.2 Å resolution

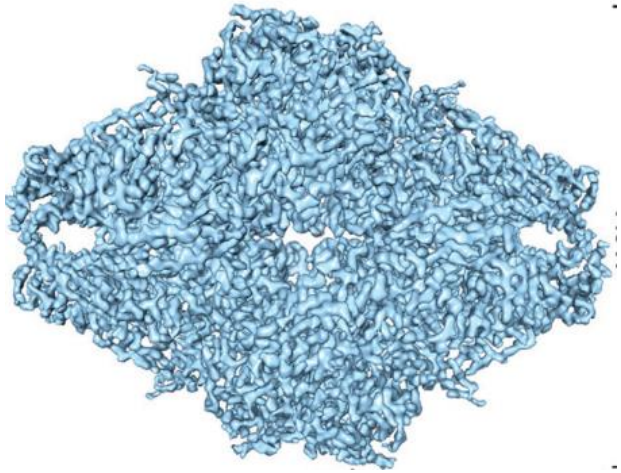

How to estimate resolution ?

- In X-ray crystallography ?
- In NMR ?
- In cryo-EM ?

How to estimate resolution ?

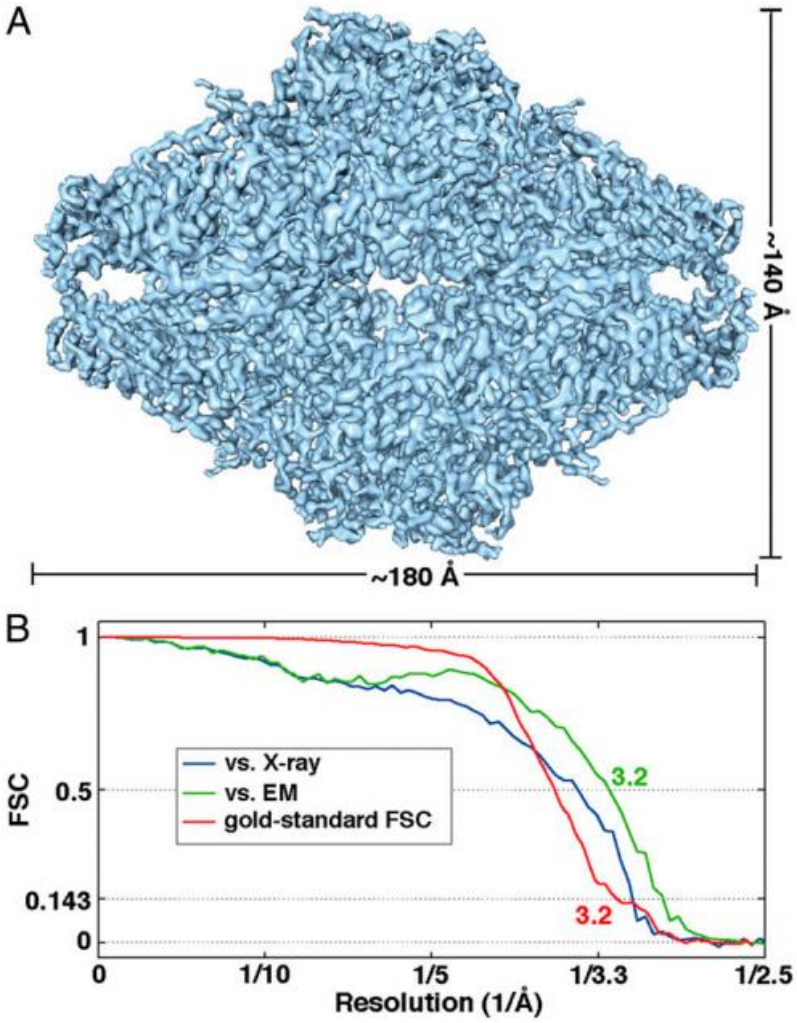

Fig. 1. Cryo-EM density map of *E. coli* β-galactosidase at 3.2-Å resolution. (*A*) Surface representation of the density map derived by cryo-EM. The dimensions of the β-galactosidase tetramer are ~180 Å x 140 Å x 87 Å. (*B*) Three different FSC plots to estimate resolution of the map shown in *A*. The curve in red shows the gold-standard FSC (24), with a value of 0.143 at 3.2-Å resolution, calculated between two independently refined halves of the dataset; the curve in blue shows the FSC (value of 0.5 at 3.6-Å resolution) calculated between the map in *A* and the map derived from the structure derived by X-ray crystallography PDB ID code 1DP0 (21); and the curve in green shows the FSC (value of 0.5 at 3.2-Å resolution) calculated between the map in *A* and the map derived from the cryo-EM–derived atomic model.

Half-maps…

Local resolution

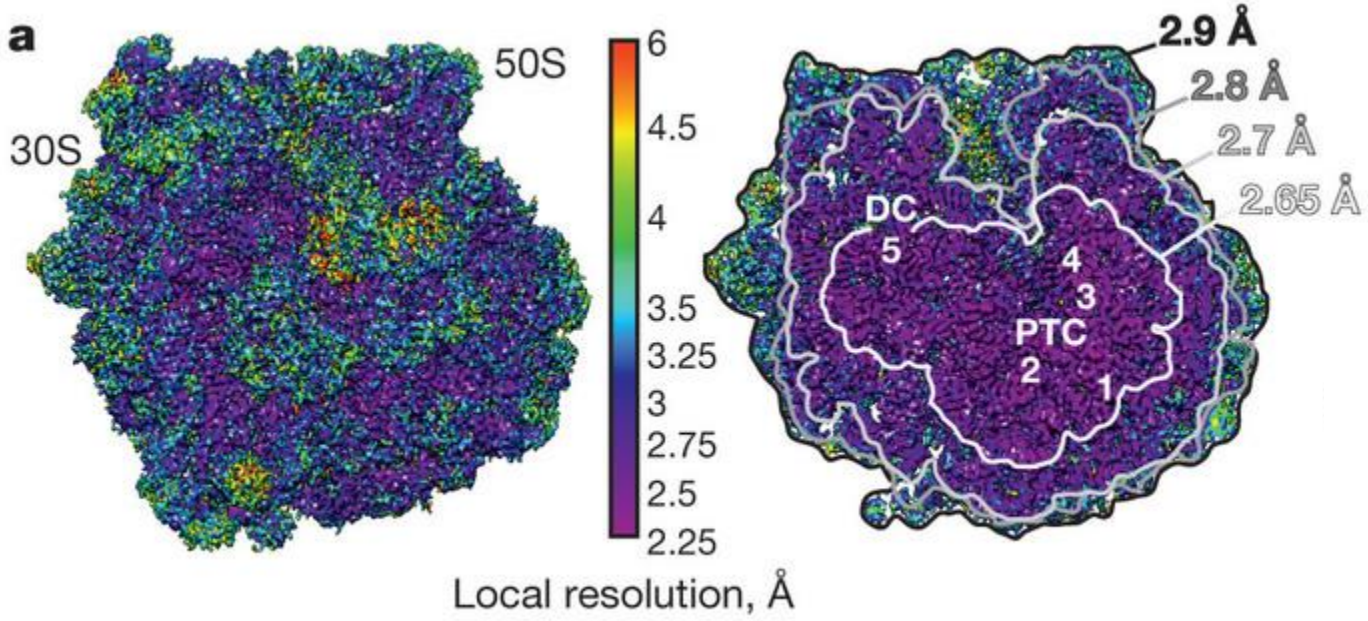

Fischer et al, 2015

How to get a high-resolution structure ?

→ Sample preparation

→Microscope imaging

→ Data processing

Microscope imaging

- Titan Krios equipped with a K2 direct electron detector mounted on a Quantum energy filter
- Data acquisition : 15s per image
- CMOS detector with 36 frames / acquisition

Relevance… ?

Compromise

- 15s : long exposure vs vibrations
- BIM correction
- Radiation damage vs contrast vs resolution

Data processing

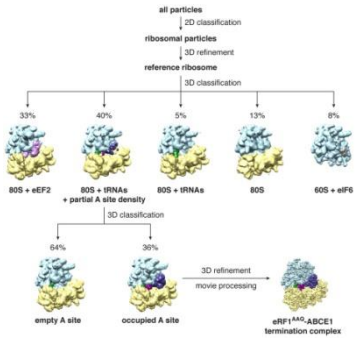

- 834 micrographs recorded (-1 to -2.5 µm)
- 509 micrographs selected
- Correction of Beam-induced motion
- CTF determination
- Resolution cutoff 3 Å

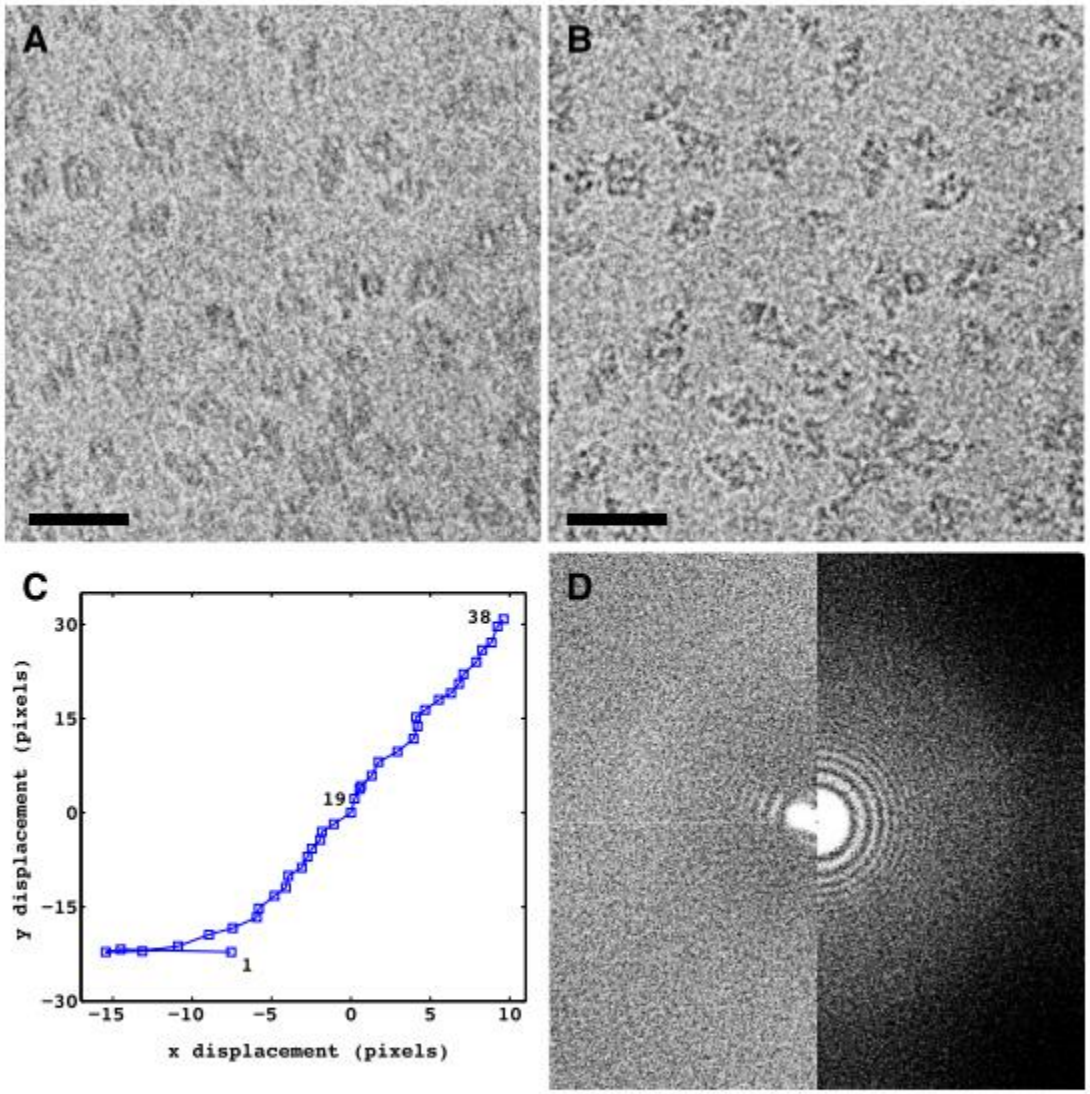

Fig. S3. Improvement in image quality obtained by aligning individual movie frames. (*A* and *B*) Comparison between averages of unaligned (*A*) and aligned (*B*) movie frames showing correction of the blurring effect caused by beam-induced motion (extreme case). (Scale bars: 25 nm.) (*C*) Trajectory of movement for each of the 38 frames during the 15.2-s exposure used in *A*. Displacements are measured in multiples of the superresolution pixel (1 pixel = 0.6375 Å). (*D*) Comparison between the FFTs of the averages of unaligned (*Left*) and aligned (*Right*) movie frames showing recovery of uniform Thon rings after correction for image movement during the exposure.

Data processing

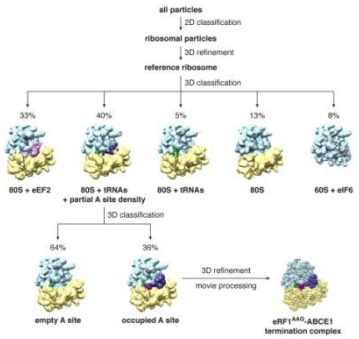

- 834 micrographs recorded (-1 to -2.5 µm)
- 509 micrographs selected
- Correction of Beam-induced motion
- CTF determination
- Resolution cutoff 3 Å

Data processing

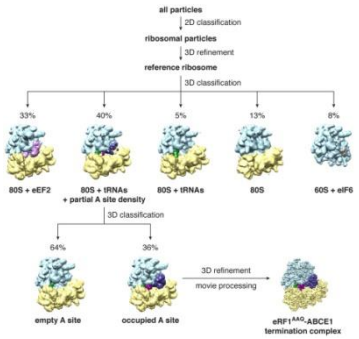

- 24 750 selected out of 509 micrographs (EMAN2)
- After 2D classification (EMAN2), 23 452 particles used in refinement (FREALIGN)
- 11 726 particles for 3D reconstruction

Conformational heterogeneity VS resolution

Final structure

- FSC cryo-EM and X-ray (resolution estimation)

Final structure

- FSC cryo-EM and X-ray (resolution estimation)
- 2/57 structures contains model N-terminal residues

Table S1. Comparison of the amino acid sequences of *E. coli* β-galactosidase encoded in expression vectors used for protein expression and the subset of the residues in the N-terminal region that are resolved and reported in the PDB entries

PDB ID code	Resolution, Å	N-terminal residues of construct used for protein expression	N-terminal residues in PDB
4DUV	2.3	MGGSHHHHHHGMASMTGGQQMGRDLYDDDDKDPMIDPVVLQRRDWENPGV	MIDPVVLQRRDWENPGV
3VD3	2.8	MGGSHHHHHHGMASMTGGQQMGRDLYDDDDKDPMIDPVVLQRRDWENPGV	RRDWENPGV
3SEP	2.1	MGGSHHHHHHGMASMTGGQQMGRDLYDDDDKDPMIDPVVLQRRDWENPGV	VVLQRRDWENPGV
3MVO	2.2	MGGSHHHHHHGMASMTGGQQMGRDLYDDDDKDPMIDPVVLQRRDWENPGV	RRDWENPGV
3MUY	2.5	GSHMLEDPVVLQRRDWENPGV	RRDWENPGV
3IAP	2.0	GSHMLEDPVVLQRRDWENPGV	RRDWENPGV
3I3E	2.0	GSHMLEDPVVLQRRDWENPGV	RRDWENPGV
3DYP	1.8	GSHMLEDPVVLQRRDWENPGV	RRDWENPGV
3EIF	3.0	GSHMLEDPVVLQRRDWENPGV	RRDWENPGV
1PX3	1.6	GSHMLEDPVVLQRRDWENPGV	RRDWENPGV
1JYX	1.5	GSHMLEDPVVLQRRDWENPGV	RRDWENPGV
1HN1	3.0	GSHMLEDPVVLQRRDWENPGV	RRDWENPGV
1F4H	2.8	ITDSLAVVLQRRDWENPGV	ITDSLAVVLQRRDWENPGV
1DP0	1.7	GSHMLEDPVVLQRRDWENPGV	RRDWENPGV
1BGL	2.5	TMITDSLAVVLQRRDWENPGV	ITDSLAVVLQRRDWENPGV

Conserved residues are underlined.

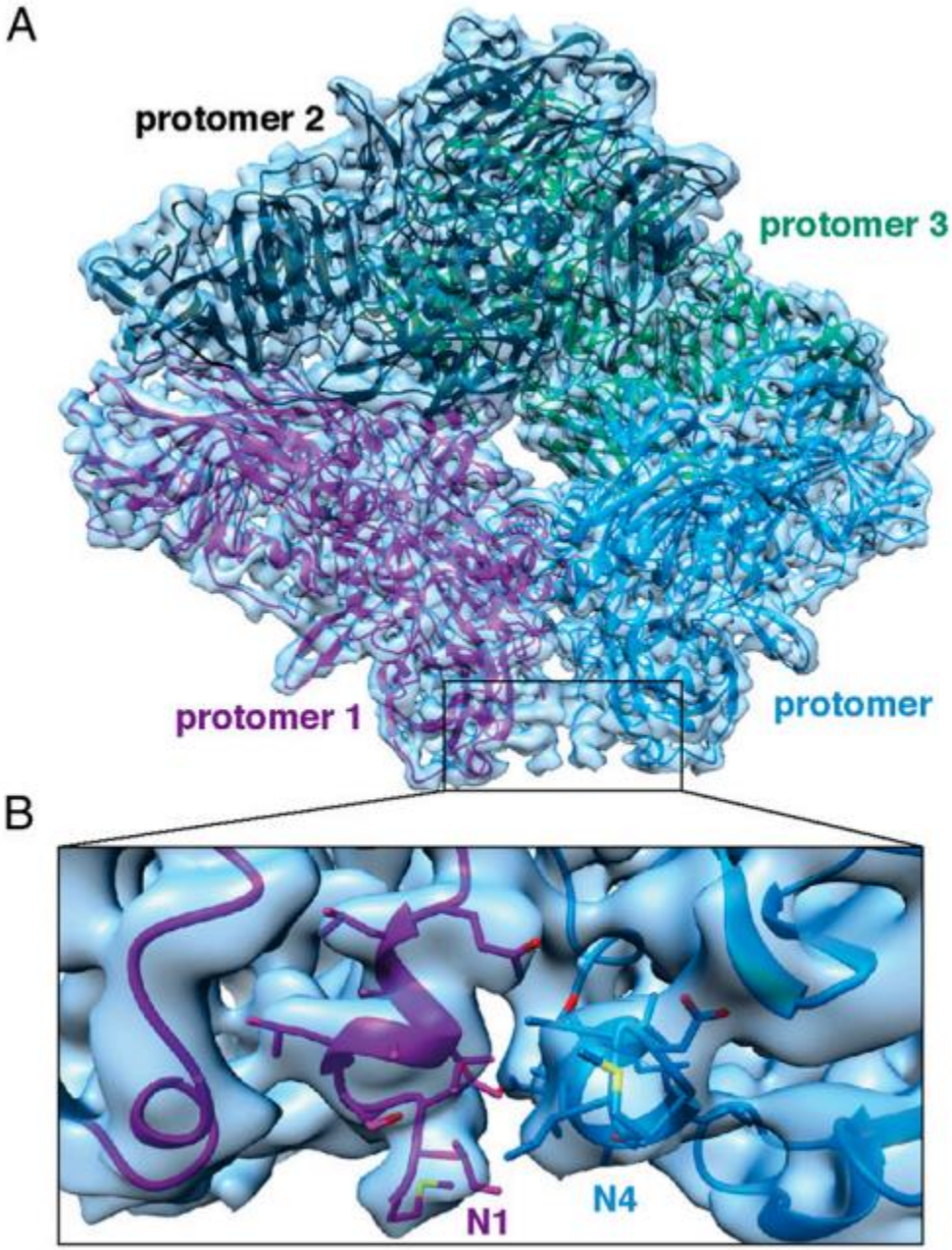

Fig. 2. Atomic model for β-galactosidase tetramer derived by cryo-EM. (*A*) Cryo-EM map shown in surface representation with fitted atomic model of β-galactosidase. The four labeled protomers are colored magenta, black, green, and blue, respectively. The density corresponding to the 12 N-terminal residues of protomers 1 and 4 are shown in the boxed region to highlight the absence of these residues in 96% of the 57 available X-ray structures. (*B*) Zoomed in region of the dimer interface highlighted in *A* showing a superposition of the cryo-EM–derived atomic model derived de novo from the experimental density map (N1 and N4 shown in magenta and blue, respectively); the cryo-EM derived atomic model closely matches that derived in the X-ray models that report coordinates for this region (only 2 of the 57 reported structures).

Final structure

- FSC cryo-EM and X-ray (resolution estimation)
- 2/57 structures contains model N-terminal residues
- Rmsd all Cα 0.66 Å vs individual Cα up to 4.6 Å

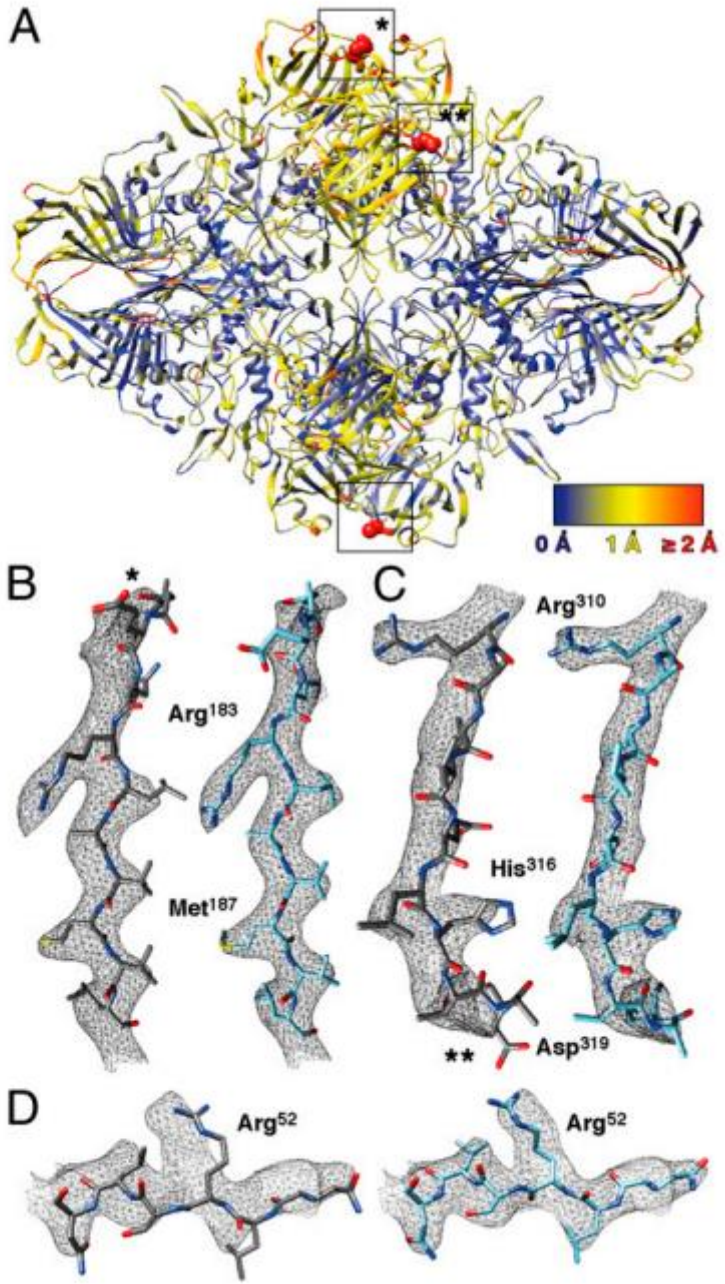

Fig. 3. Comparison of atomic models of *E. coli* β-galactosidase derived by X-ray crystallography at 1.7-Å resolution and by cryo-EM at 3.2-Å resolution. (*A*) X-ray structure of *E. coli* β-galactosidase (PDB ID code 1DP0; ref. 21) after alignment to the cryo-EM structure shown in ribbon representation colored according to rmsd values [ranging from blue (low) to red (high)]. Each chain was aligned separately in Chimera, using the default algorithm (Needleman–Wunsch in BLOSUM-62 Matrix). Highlighted areas shown as red spheres correspond to regions marked with asterisks (* and **) with rmsd values for Cα over 2 Å that are involved in crystal contacts (Fig. S9). (*B–D*) Local deviations between the atomic model derived from X-ray crystallography (*Left* in gray sticks) and the atomic model derived from cryo-EM (*Right* in light blue sticks) superimposed on the cryo-EM density map (mesh representation). Zones of protein-protein contacts in the crystal lattice including residues 179–189 (marked * in *A*) are shown in *B*, and the region including residues 310–320 (marked ** in *A*) is shown in *C*. Example of local deviations near residues 50–55, which are not involved in crystal contacts but located at the periphery of the enzyme is shown in *D*. In all examples, displacement of side chains and the backbone regions is visible.

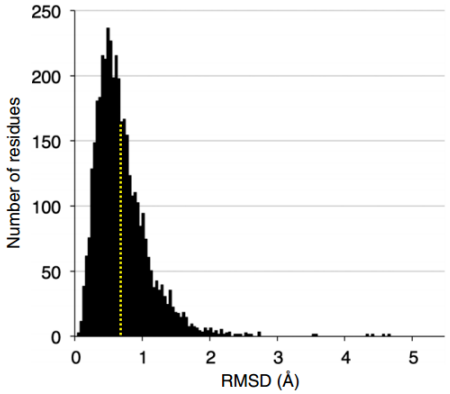

Fig. S8. Histogram showing the distribution of rmsd values of individual Cα atoms between corresponding residues in the cryo-EM and X-ray (PDB ID code 1DP0) structures. Values range between 0.04 and 4.64 Å, with an average of 0.66 Å (yellow dashed line).

Final structure

- FSC cryo-EM and X-ray (resolution estimation)
- 2/57 structures contains model N-terminal residues
- Rmsd all Cα 0.66 Å vs individual Cα up to 4.6 Å
- Crystal contacts

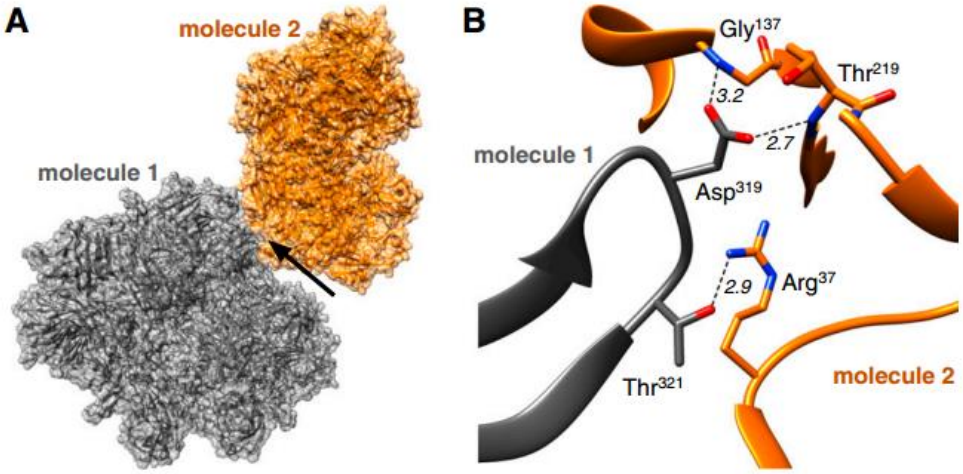

Fig. S9. Residues involved in crystal contacts. (*A*) Visualization of one of the crystal contacts (region ** in Fig. 3) highlighting the intermolecular interaction (indicated by the arrow) of two β-gal tetramers (shown in gray and orange) in the 3D crystal lattice (PDB ID code 1DP0). The presence of this crystal contact correlates with the difference in local backbone conformation between the crystal and cryo-EM structures. (*B*) Detailed view of the interaction between a peripheral loop from one tetramer (shown in gray) with three distinct regions on the neighboring tetramer in the crystal lattice.

Final structure

- FSC cryo-EM and X-ray (resolution estimation)
- 2/57 structures contains model N-terminal residues
- Rmsd all Cα 0.66 Å vs individual Cα up to 4.6 Å
- Crystal contacts
- Side chains well resolved (even long side chains)

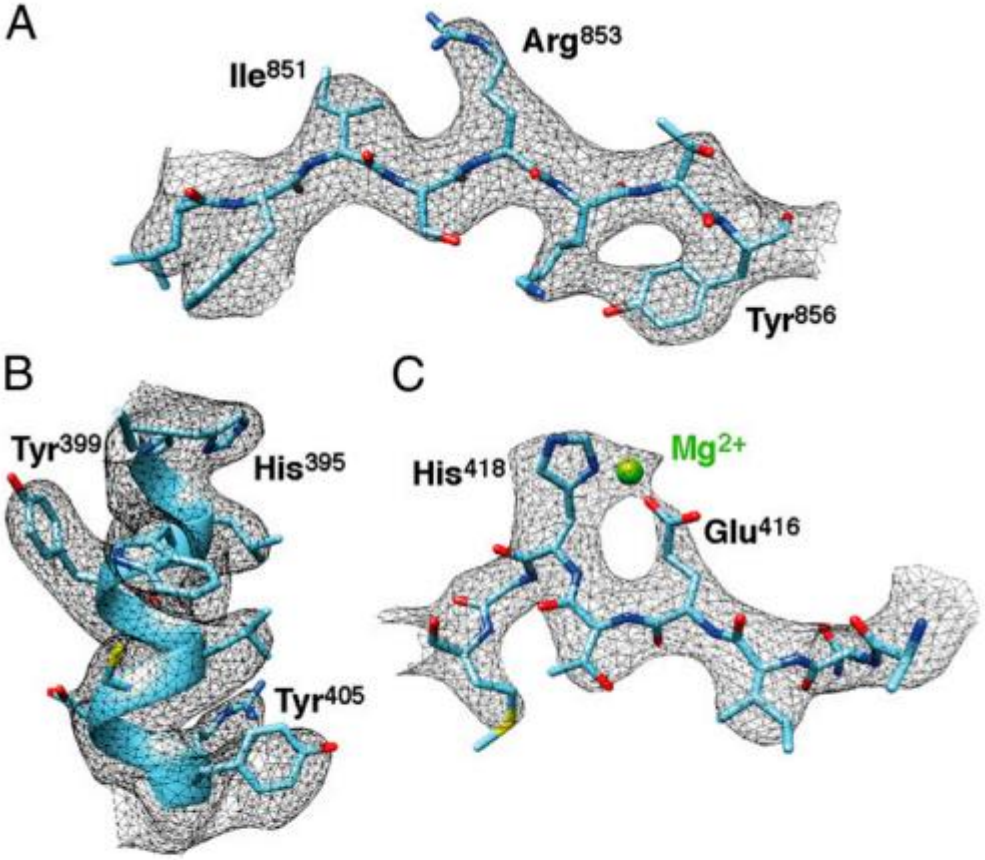

Fig. 4. Quality of cryo-EM–derived density map. Selected regions showing the fit of the derived atomic model to the cryo-EM density map (black mesh). Residues 849–856 in a β-strand (*A*), residues 395–405 in an α-helix (*B*), and residues 413–420 in the active site along with density for a Mg^{2+} ion partly coordinated by His-418 and Glu-416 (*C*).

Final structure

- FSC cryo-EM and X-ray (resolution estimation)
- 2/57 structures contains model N-terminal residues
- Rmsd all Cα 0.66 Å vs individual Cα up to 4.6 Å
- Crystal contacts
- Side chains well resolved (even long side chains)
- Negative side chains are weaker (other example)

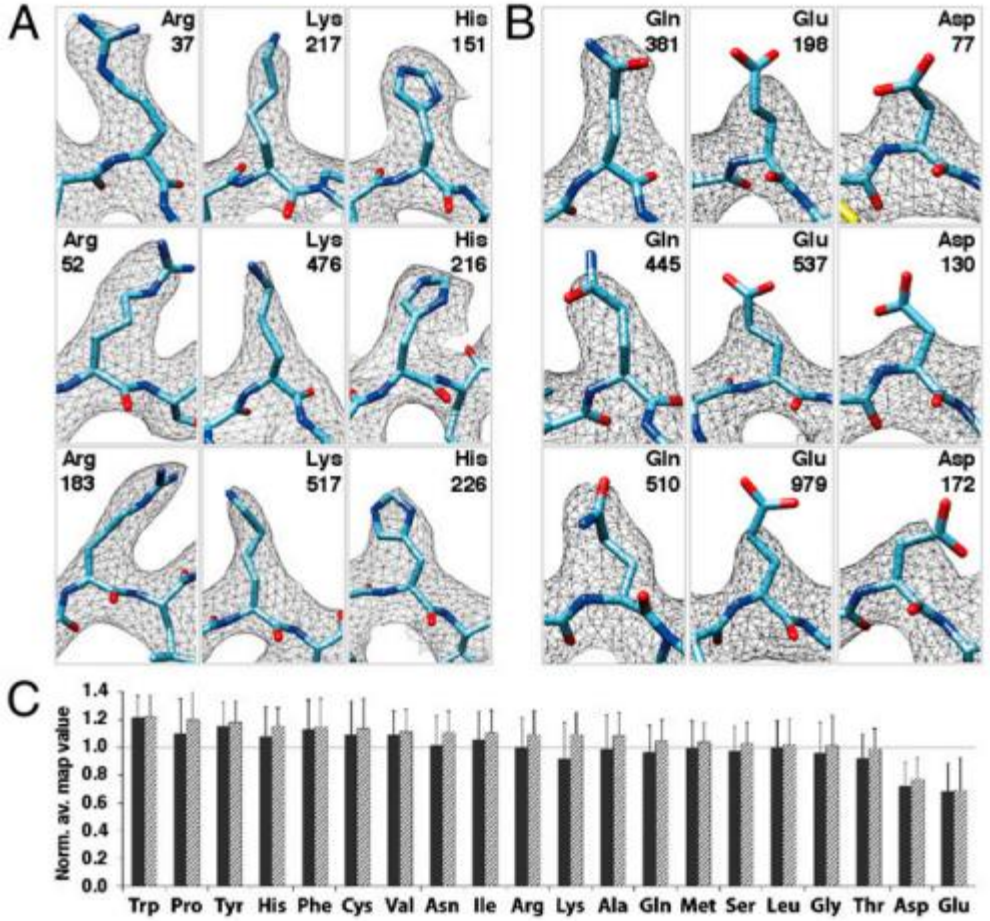

Fig. 5. Variation in observed side-chain densities between different types of residues. (*A*) Densities observed for a set of Arg, Lys, and His residues (shown in stick representation). (*B*) Comparison of densities observed for a set of Gln and Glu residues, as well as Asp residues to indicate preferential loss of density for the negatively charged side chains in comparison with the similarly sized, but neutral side chains. (*C*) Plot of normalized averaged map values (as detailed in Fig. S12), shown for each residue type when only buried residues are considered (hatched bars) or when all residues including buried and exposed varieties are considered (filled bars). Buried residues are defined as those where <30% of their maximum possible surface area is exposed to solvent.

Final structure

- FSC cryo-EM and X-ray (resolution estimation)
- 2/57 structures contains model N-terminal residues
- Rmsd all Cα 0.66 Å vs individual Cα up to 4.6 Å
- Crystal contacts
- Side chains well resolved (even long side chains)
- Negative side chains are weaker (other example)
- Radiation damage : test at 10, 20 or 30 $e^-/ Å^2$

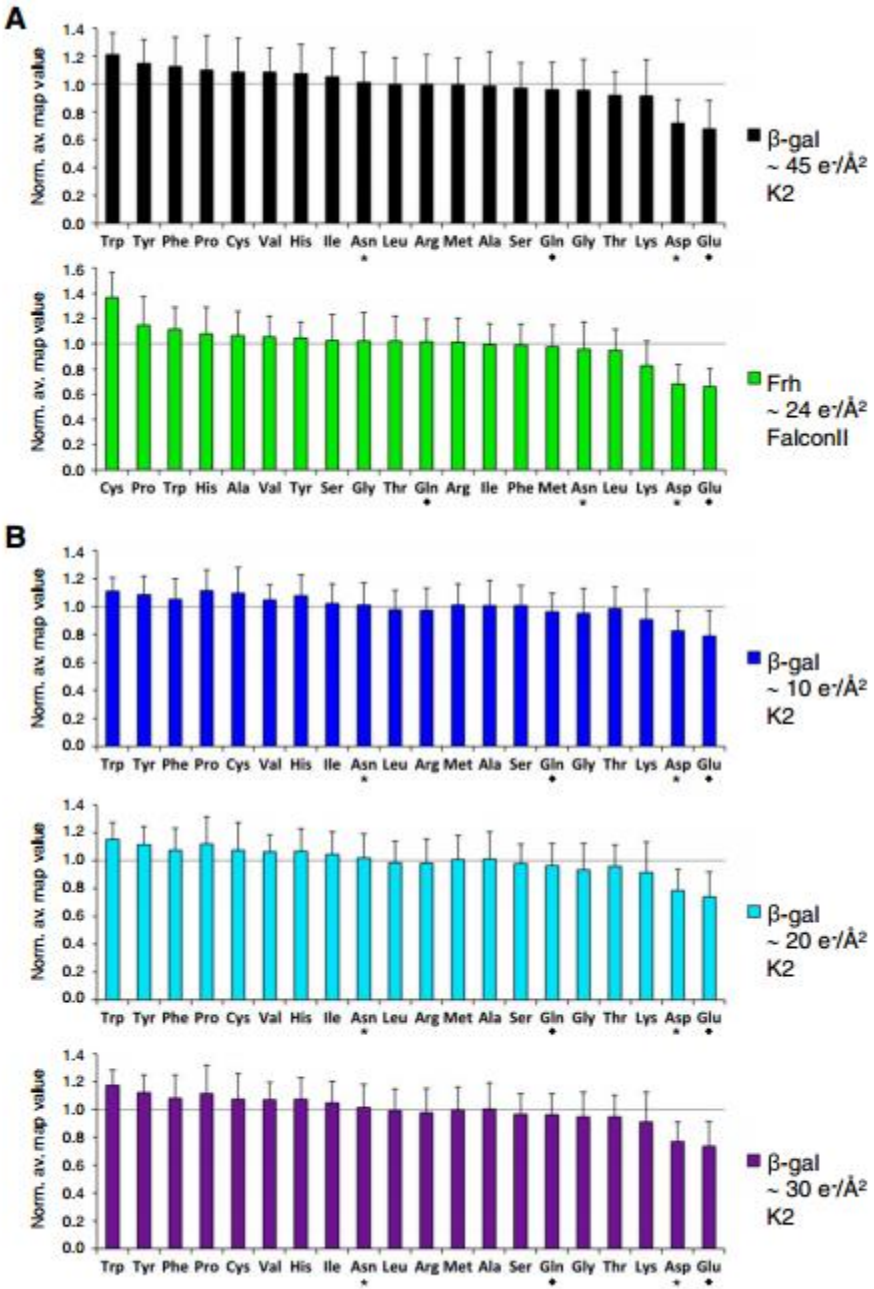

Fig. S12. Proportional variation in side-chain density measured for each residue type on different cryo-EM maps. (*A*) Plots of normalized average map values for each type of residue for the ~3.2-Å map of β-galactosidase (β-gal, *Upper*, black) and the 3.36-Å map of F$_{ox}$-reducing [NiFe] hydrogenase (1) (Frh, *Lower*,

What did we learn from cryo-EM ?

- Cryo-EM can be used as a powerful technique to get high resolution structures
- Conformation in crystal vs solution
- Local resolution (dynamics)
- Drawbacks : radiation damage, dose vs contrast vs resolution

Tricks

- What tricks should we use to get to a higher resolution structure ?

Journal club cryo-EM

PNAS

Structure of β-galactosidase at 3.2-Å resolution obtained by cryo-electron microscopy

Alberto Bartesaghi[1], Doreen Matthies[1], Soojay Banerjee, Alan Merk, and Sriram Subramaniam[2]

Laboratory of Cell Biology, Center for Cancer Research, National Cancer Institute, National Institutes of Health, Bethesda, MD 20892

Edited by Wah Chiu, Baylor College of Medicine, Houston, TX, and approved June 20, 2014 (received for review February 14, 2014)

We report the solution structure of *Escherichia coli* β-galactosidase (~465 kDa), solved at ~3.2-Å resolution by using single-particle cryo-electron microscopy (cryo-EM). Densities for most side chains, including those of residues in the active site, and a catalytic Mg^{2+} ion can be discerned in the map obtained by cryo-EM. The atomic model derived from our cryo-EM analysis closely matches the 1.7-Å crystal structure with a global rmsd of ~0.66 Å. There are significant local differences throughout the protein, with clear evidence for conformational changes resulting from contact zones in the crystal lattice. Inspection of the map reveals that although densities for residues with positively charged and neutral side chains are well resolved, systematically weaker densities are observed for residues with negatively charged side chains. We show that the weaker densities for negatively charged residues arise from their greater sensitivity to radiation damage from electron irradiation as determined by comparison of density maps obtained by using electron doses ranging from 10 to 30 $e^-/Å^2$. In summary, we establish that it is feasible to use cryo-EM to determine near-atomic resolution structures of protein complexes (<500 kDa) with low symmetry, and that the residue-specific radiation damage that occurs with increasing electron dose can be monitored by using dose fractionation tools available with direct electron detector technology.

Science AAAS

ELECTRON MICROSCOPY

2.2 Å resolution cryo-EM structure of β-galactosidase in complex with a cell-permeant inhibitor

Alberto Bartesaghi,[1]* Alan Merk,[1]* Soojay Banerjee,[1] Doreen Matthies,[1] Xiongwu Wu,[2] Jacqueline L. S. Milne,[1] Sriram Subramaniam[1]†

Cryo–electron microscopy (cryo-EM) is rapidly emerging as a powerful tool for protein structure determination at high resolution. Here we report the structure of a complex between *Escherichia coli* β-galactosidase and the cell-permeant inhibitor phenylethyl β-D-thiogalactopyranoside (PETG), determined by cryo-EM at an average resolution of ~2.2 angstroms (Å). Besides the PETG ligand, we identified densities in the map for ~800 water molecules and for magnesium and sodium ions. Although it is likely that continued advances in detector technology may further enhance resolution, our findings demonstrate that preparation of specimens of adequate quality and intrinsic protein flexibility, rather than imaging or image-processing technologies, now represent the major bottlenecks to routinely achieving resolutions close to 2 Å using single-particle cryo-EM.

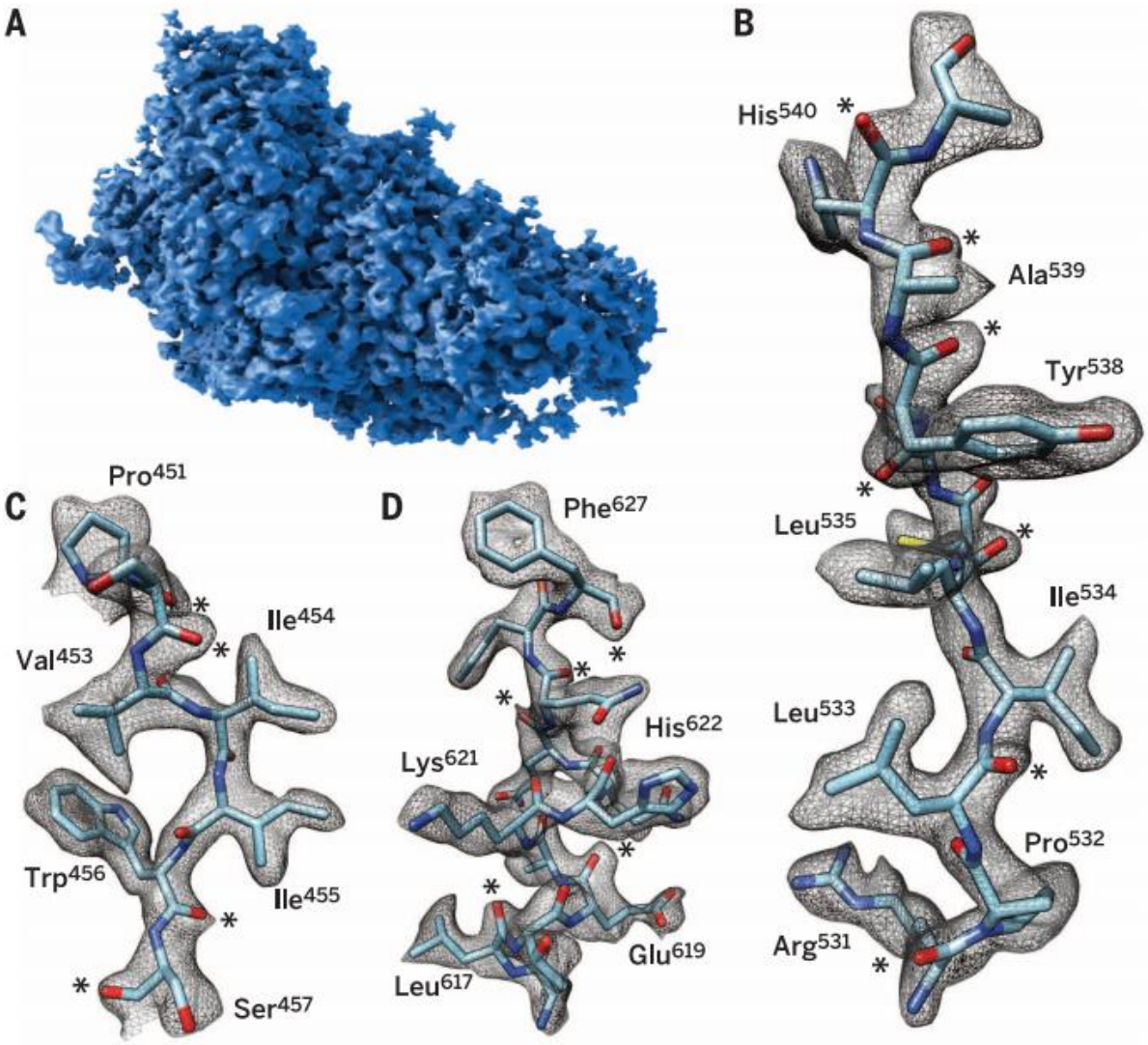

Fig. 1. Cryo-EM density map of the β-Gal–PETG complex at 2.2 Å resolution. (**A**) Surface representation of the density map of one of the four protomers in the tetrameric complex. (**B** to **D**) Visualization of selected map regions showing delineation of secondary structural elements, amino acid densities, and carbonyl moieties (indicated by asterisks). The density for Phe^{627} is thinned out in the center of the aromatic ring, revealing the presence of a "hole" in the ring, a feature typically observed in structures determined by x-ray crystallography at resolutions of ~2 Å.

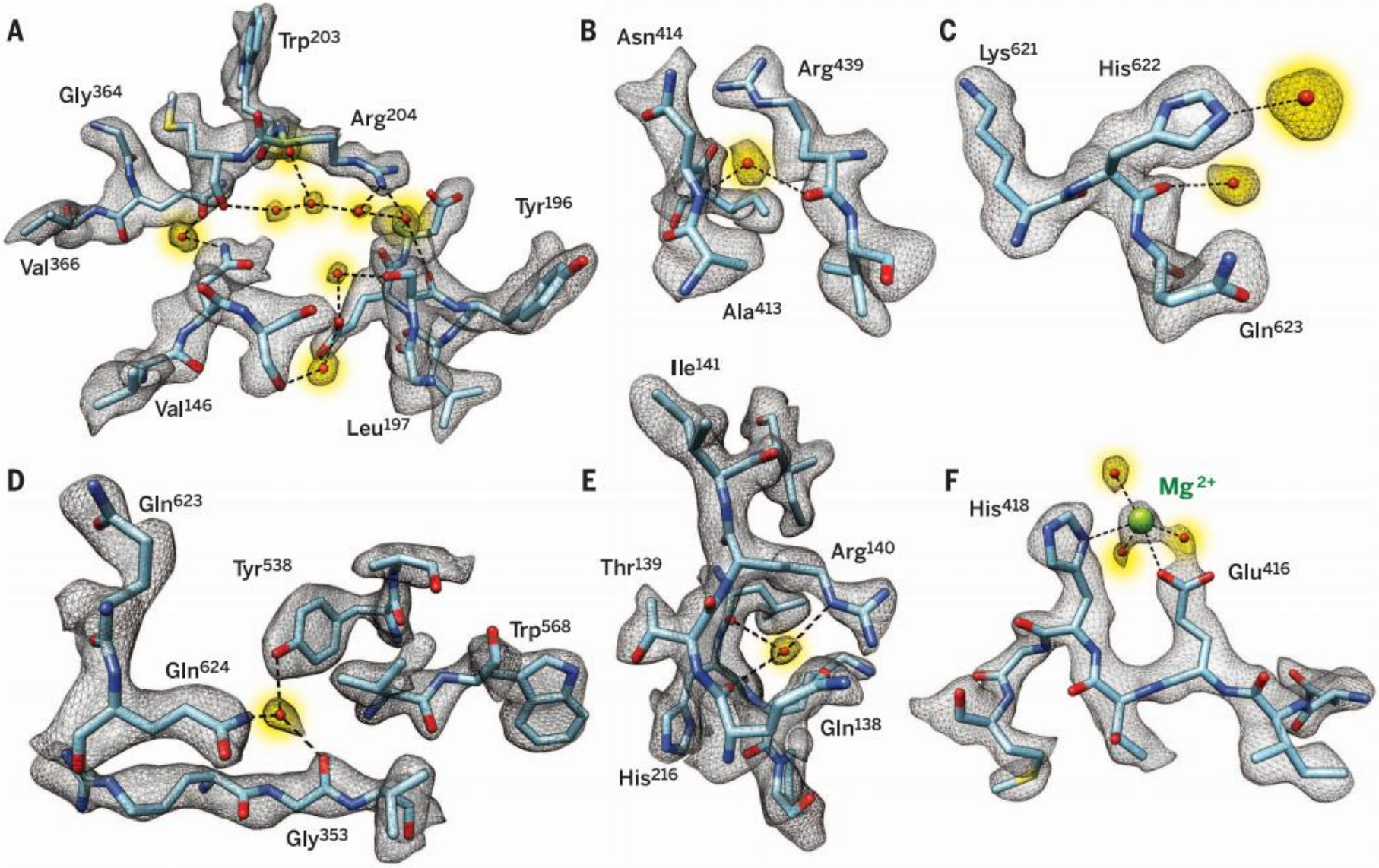

Fig. 2. Visualization of tightly bound water molecules in the structure of the β-Gal–PETG complex. (**A** to **F**) Selected examples of densities for water molecules (highlighted in yellow) hydrogen bonded in pearl-string–like chains (A), connected to the polypeptide backbone and multiple amino acid side chains [(B) to (E)], or interacting with the Mg^{2+} ion in the active site (F).

Fig. 3. Active-site structure in PETG-liganded *E. coli* β-Gal. (**A**) Uncorrected cryo-EM density map showing density for PETG, an associated water molecule, and six of the amino acids that line the binding pocket. (**B**) Plot of distances of various parts of PETG to residues in the vicinity of β-Gal from *E. coli*, determined using LIGPLOT (www.ebi.ac.uk/thornton-srv/software/LIGPLOT/). (**C**) Superposition of the ligand binding pocket structures in β-Gal from *E. coli* (light blue, determined by cryo-EM at 2.2 Å resolution) and *T. reesei* (green, determined by x-ray crystallography at 1.4 Å resolution), illustrating the differences in protein and ligand structures. (Inset) Comparison between the corresponding configurations of PETG. (**D**) Plot of distances of various parts of PETG to amino acids in the vicinity of β-Gal from *T. reesei*, determined using LIGPLOT.

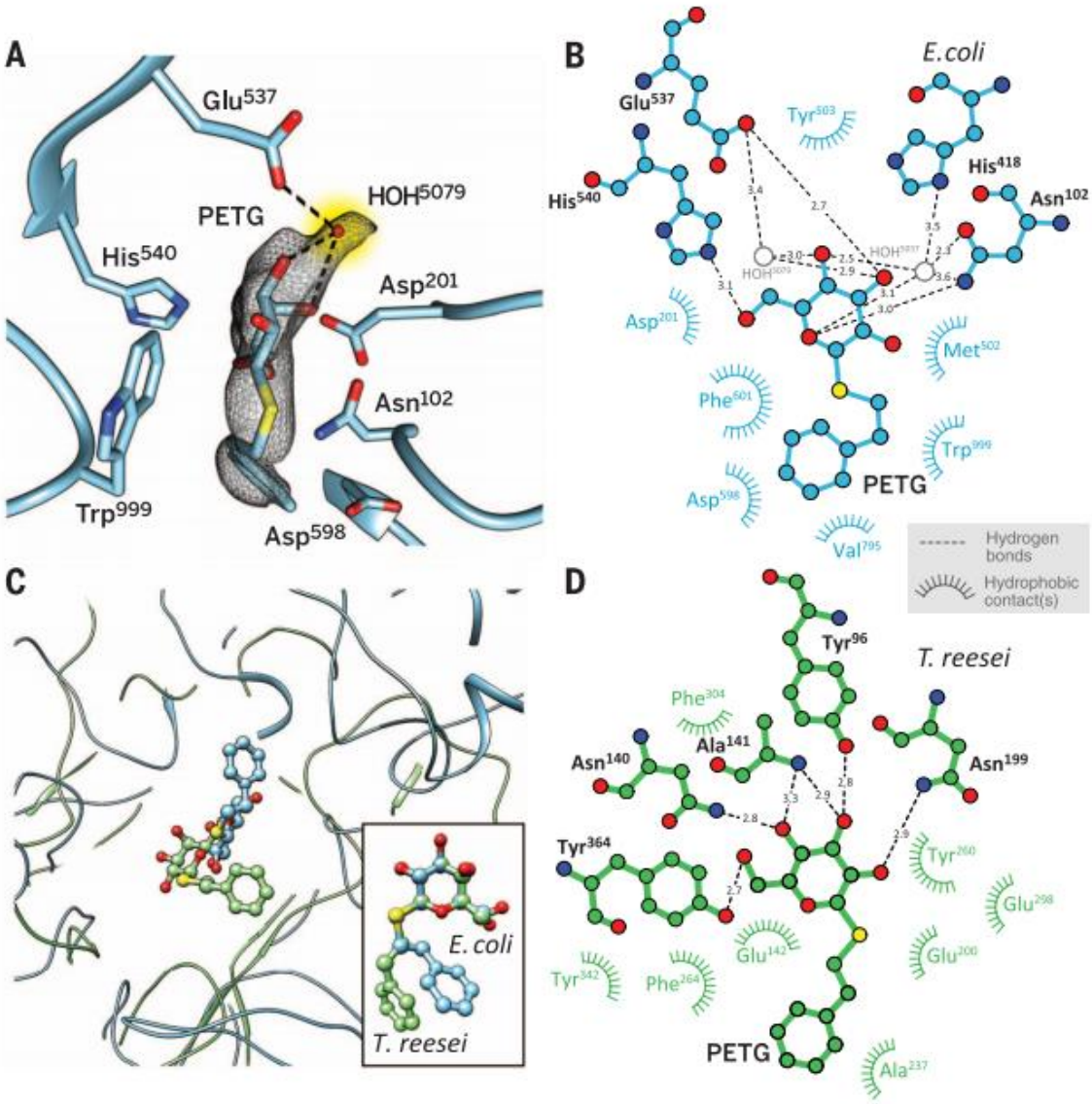

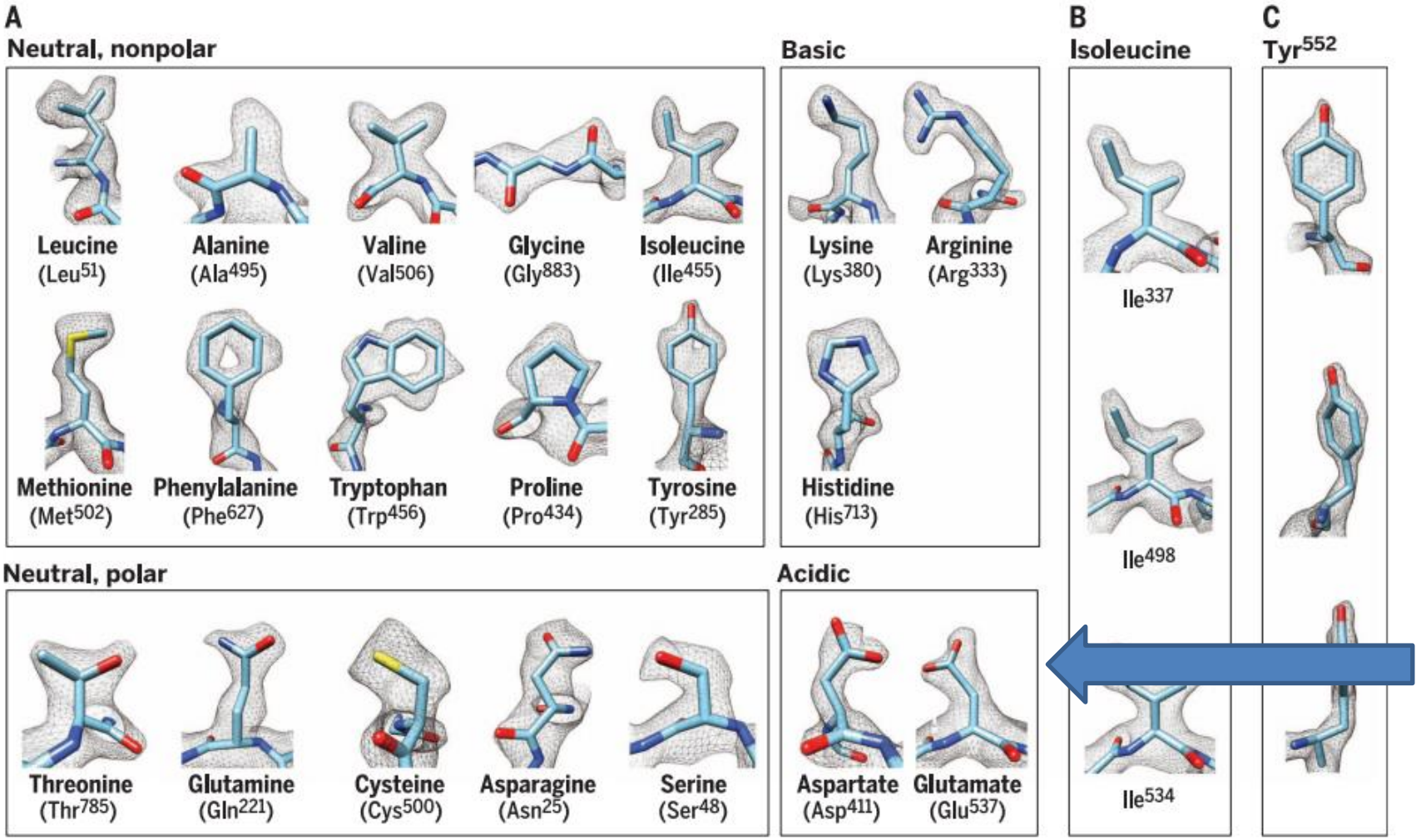

Fig. 4. Illustration of map quality at the level of amino acids. (**A**) Visualization of map density for examples of each of the 20 standard amino acids, which are grouped into neutral (nonpolar and polar), basic, and acidic categories. (**B** and **C**) Illustration of contours of densities for multiple Ile residues (B) and front, tilted, and edge views for Tyr^{552} (C). In each case, the density contours are consistent with the 2.2 Å resolution we report.

How to get a high-resolution structure ?

→ Sample preparation

→Microscope imaging

→ Data processing

Stabilization – Fab fragments or ligands

Vs

conformation heterogeneity

How to get a high-resolution structure ?

→ Sample preparation

→Microscope imaging

→ Data processing

8s exposure

How to get a high-resolution structure ?

→ Sample preparation

→Microscope imaging

→ Data processing

Data processing

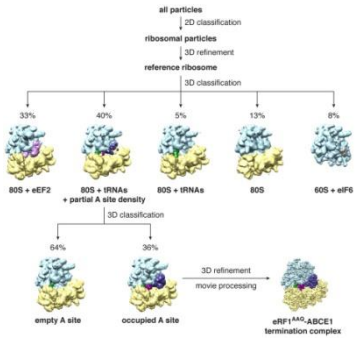

- Selection of images : 1487 recorded
- Signal over 3 Å
- 93 686 particles
- Frames selection
- Best : 12 $e^-/Å^2$
- 3D classification !!!
- 194 water molecules / monomer (same as X-ray) !!
- Distortions : inaccuracies in determination of the CTF of each image, errors in orientation determination during refinement, distinct patterns of radiation damage, uniform B-factor correction to scale the map

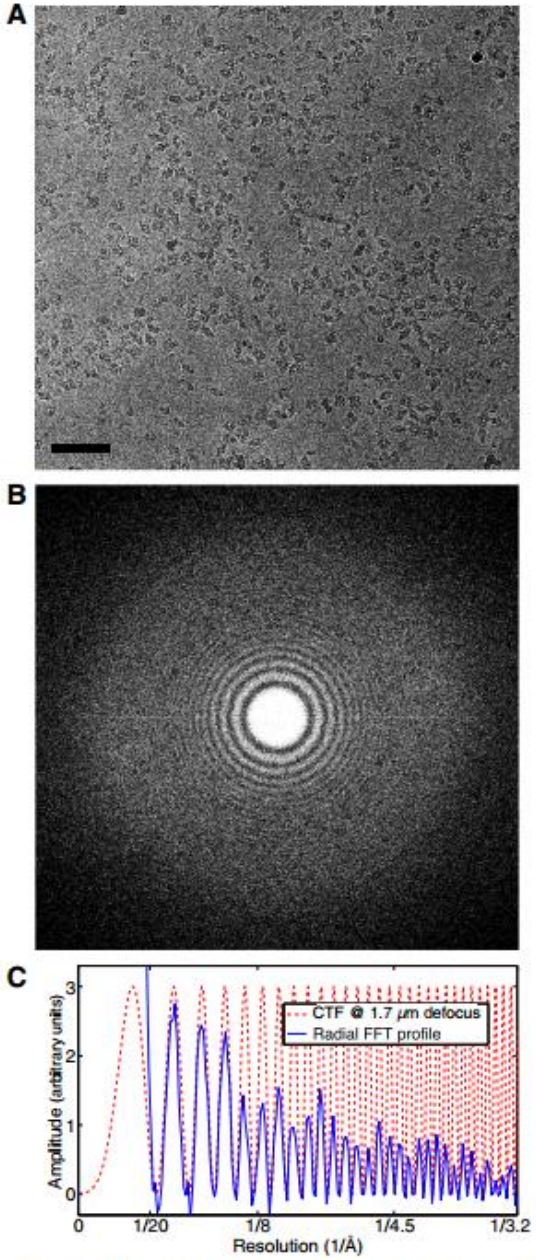

Fig. S1. Cryo-EM of *Escherichia coli* β-galactosidase. (*A*) Average of 38 aligned movie frames acquired over a 15.2-s exposure window (45 $e^-/Å^2$ total accumulated dose) with images recorded at 300 kV and −1.7 μm defocus in superresolution mode by using a physical pixel size of 1.275 Å. (Scale bar: 50 nm.) (*B*) Fast Fourier transform (FFT) of image in *A* showing the extent of Thon rings present in the data extending to ~2/3 of the edge of the transform, which corresponds to 2.55 Å. (*C*) One-dimensional power spectrum profile obtained by radially averaging the Fourier transform of the image in *A*; peaks are clearly visible out to 3.2-Å resolution.

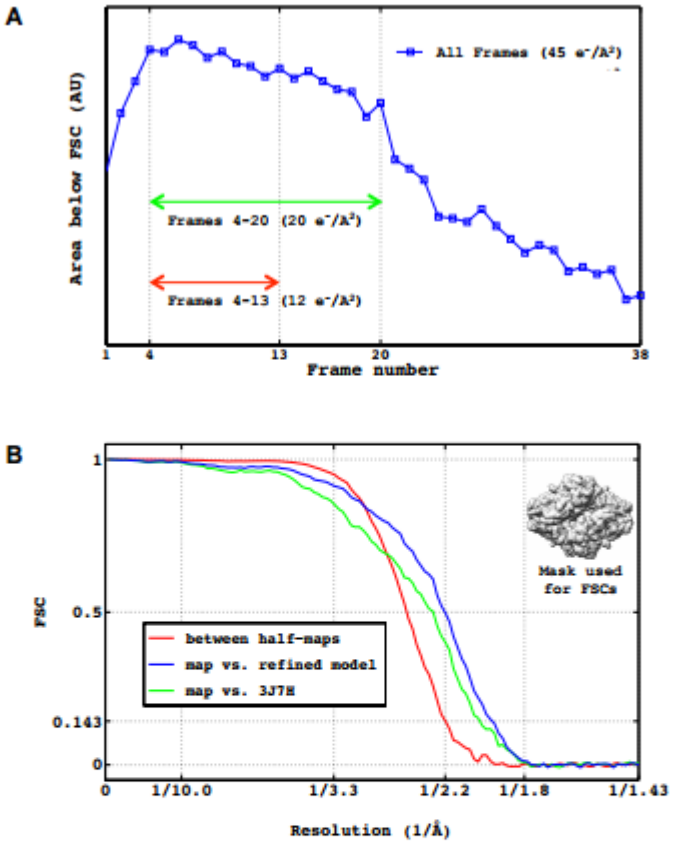

Fig. S3

Assessment of resolution and contribution of individual frames to the cryo-EM density map of β-galactosidase-PETG complex at 2.2 Å resolution. **(A)** Contribution of individual frames to the density map measured by integrating the FSC curves between maps obtained from the individual frames and the map obtained using all the frames. From a total of 38 frames, the average of frames 4-20 (the least affected by beam-induced motion and radiation damage) was used for 3D refinement, and the average of frames 4-13 (containing the highest resolution information) was used to obtain the final reconstruction shown in Figs. 1-4. **(B)** Fourier Shell Correlation (FSC) curve between two semi-independently refined halves of the data (red curve) and FSC plot calculated between the map shown in Figs. 1-4 and the map computed from the cryo-EM-derived atomic model (blue curve) both showing a resolution value of ~ 2.2 Å at the 0.143 and 0.5 cutoffs, respectively. For comparison, the corresponding plot derived using our earlier structure of apo β-galactosidase at 3.2 Å resolution (PDB 3J7H) is also shown (green curve). All FSC calculations were done using the soft shape mask illustrated in the inset.

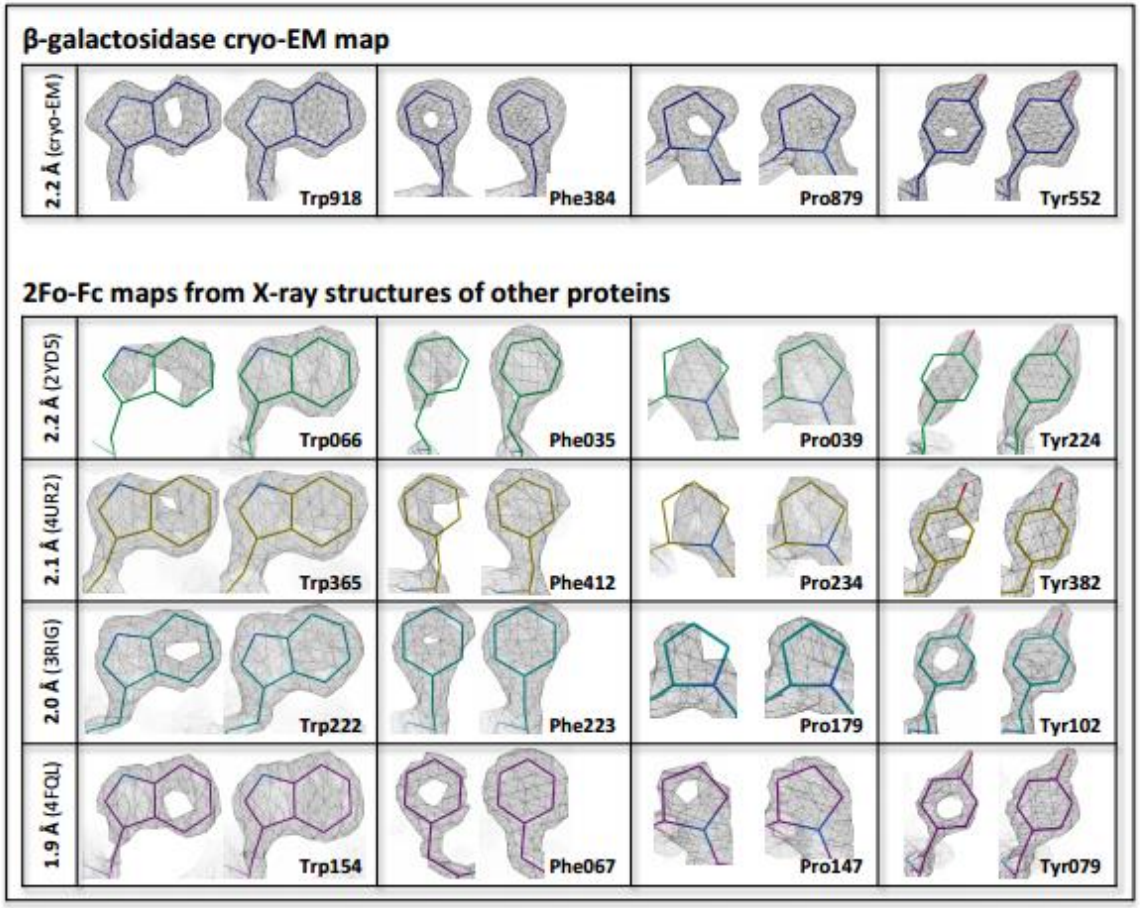

Fig. S4

Comparison of densities visualized for four residue types in the experimentally determined cryo-EM map of β-galactosidase at an overall resolution of 2.2 Å, with 2Fo-Fc maps from previous X-ray structures at resolutions ranging from 1.9 Å to 2.2 Å. Density for residues Trp, Phe, Tyr and Pro are contoured at two different levels (columns 1 and 2). Raw cryo-EM map (first row), PDB 2YD5 at 2.2 Å resolution (*30*), PDB 4UR2 at 2.1 Å resolution (*31*), PDB 3RIG at 2.0 Å resolution (*32*), and PDB 4FQL at 1.9 Å resolution (*33*). The appearance of densities in our map is comparable to features observed in X-ray maps at resolutions ranging from 1.9 to 2.2 Å. The holes in Trp, Phe and Tyr that are visible in our cryo-EM map are visible in the X-ray structures at 2.1 Å or better, while the holes in Pro visible in our map are visible in the X-ray structures at 2.0 Å or better.

Distortions in density

Cryo-EM : a good compromise

→ Sample preparation

→Microscope imaging

→ Data processing

Chromatography, ligands, gif, CMOS, data processing…

Questions